Chapter

Scale Invariant Turbulence and Gibbs Free Energy in the Atmosphere

Adrian F. Tuck

Abstract

A method of calculating the Gibbs Free Energy (Exergy) for the Earth's atmosphere using statistical multifractality — scale invariance - is described, and examples given of its application to the stratosphere, including a methodology for extension to aerosol particles. The role of organic molecules in determining the radiative transfer characteristics of aerosols is pointed out. These methods are discussed in the context of the atmosphere as an open system far from chemical and physical equilibrium, and used to urge caution in deploying "solar radiation management".

Keywords: scale invariance, entropy, exergy, atmosphere

1. Introduction

Earth's atmosphere is an open system far from equilibrium, both physically – there is vigorous circulation, and chemically – for example, the methane/oxygen ratio is some 30 orders of magnitude larger than the equilibrium value. It is not isolated; there are varying fluxes of photons in and out, water exchanges on a 10-day time scale with the oceans, carbon dioxide, many organic molecules, nitrous oxide, methane, methyl chloride, ammonia and sulphurous compounds are subject to biogeochemistry at both land and sea surfaces. Long-lived molecules such as chlorofluoromethanes (50–100 years) can be re-emitted from both land and sea, and even the major constituents, O_2 (order 10^4 years) and N_2 (order 10^6 years) are cycled by geochemistry, biochemistry and lightning. Last but not least, condensed matter in the form of aqueous aerosols is produced by gas to particle conversion, by clouds and from sea spray, and which serve as condensation nuclei for cloud droplets, ice crystals and precipitation. The air-water interface is an important reaction venue [1], and often accelerates reactions [2–6]. Some or all of these molecules and particles affect the transmission of both solar visible and ultraviolet and terrestrial infrared radiation, and consequently are central to the maintenance of atmospheric temperature.

Since the atmosphere is so far from equilibrium, standard statistical thermodynamics calculable by quantal chemical techniques are not applicable, either in the air or aerosols. The thermodynamic formulation of statistical multifractals has been shown to be a mapping, not just a formal coincidence by Lovejoy and Schertzer [7], following their analyses of atmospheric variables as statistical multifractals [8, 9]. It has been used to demonstrate, by analysis of observations, that the current global

heating is attributable almost wholly to carbon dioxide emissions from fossil fuel burning [10]. Note that this is a numerical model-independent result. By combining these analyses with results from molecular dynamics calculations [11] it has been shown that atmospheric turbulence is an emergent property of molecular gas populations in an asymmetric environment, scale invariant over the 15 orders of magnitude in length scale, from the mean free path at surface pressure to a great circle [5, 12, 13]. The scale invariance approach to atmospheric thermodynamics has been successfully applied to aircraft data from the stratosphere [14] and combined with theoretical and experimental results for aerosol particles to form a potential pathway to understanding and exploiting the observed acceleration of many chemical reactions, some of them atmospheric chemical, in and on microdroplets compared to their slower or non-occurrent behaviour in bulk fluid [5]. Microdroplet surfaces are where free energy is concentrated, even in a pure homogeneous droplet, as surface tension. So, for both gaseous composition chemistry and the aerosol population, analysis can be attempted with this approach. All these factors are directly relevant to the calculation of global heating under anthropogenic perturbations. The issue is examined in the rest of the chapter by this scale invariant thermodynamics approach. A useful review of energy production and its interaction with the environment is given in Goede et al. [15]. Further considerations are in Refs. [16–18].

The above approach provides perspective on geoengineering by "solar radiation management" when combined with the complexities of aerosol particles in the lower stratosphere [19]. Because of dissipation by infrared radiation to space, any method of reducing global heating by fossil fuel burning cannot be powered by combustion of coal, oil and gas: renewable sources must be deployed.

2. Atmospheric entropy and Gibbs free energy from scale invariance

This account draws on those in Tuck [5, 12–14, 17, 19] and references therein. In order to maintain scale invariance, the same processes must be at work scale by scale over the range concerned, 40 metres to a great circle (40,000 km) in this case. That process is manifest as turbulence, driven by the thermodynamic need to minimise Gibbs free energy, which it does by dilution of energy density. **Figure 1** shows an example of an airborne temperature trace at 200 m resolution. Analyses for the scaling exponent H and the intermittency C_1 are also shown, see below for definitions.

Satellite data have extended the aircraft data's range from an Earth radius to a circumference [16]. A view of the atmospheric circulation then emerges wherein organised flow, the general circulation, is driven by turbulence that enables the minimisation of Gibbs free energy. That free energy arises from the absorption of photons from the low entropy solar beam by ozone, some clouds, a little by water vapour and by the surface. The necessary dissipation is achieved by infrared radiation to space from water vapour, carbon dioxide, ozone, water dimers, nitrous oxide, methane and assorted halocarbons. Radiation of both solar and terrestrial photons is by gases whose fluctuating abundance is modulated by atmospheric turbulence. The radiative effect of aerosols and clouds, including absorption, emission and scattering is an important component in the radiative balance, and the abundances of both are also modulated by turbulence.

Why turbulence? Is a question addressed successively by Horace Lamb, Théodore von Kármán and Werner Heisenberg, all of whom anticipated a disappointment in or hope for divine enlightenment upon entry to heaven – possibly with a Shakespearean degree of irony. Richard Feynman described it as the last unsolved major problem in classical physics. Here the view is put forward that it is an emergent property of

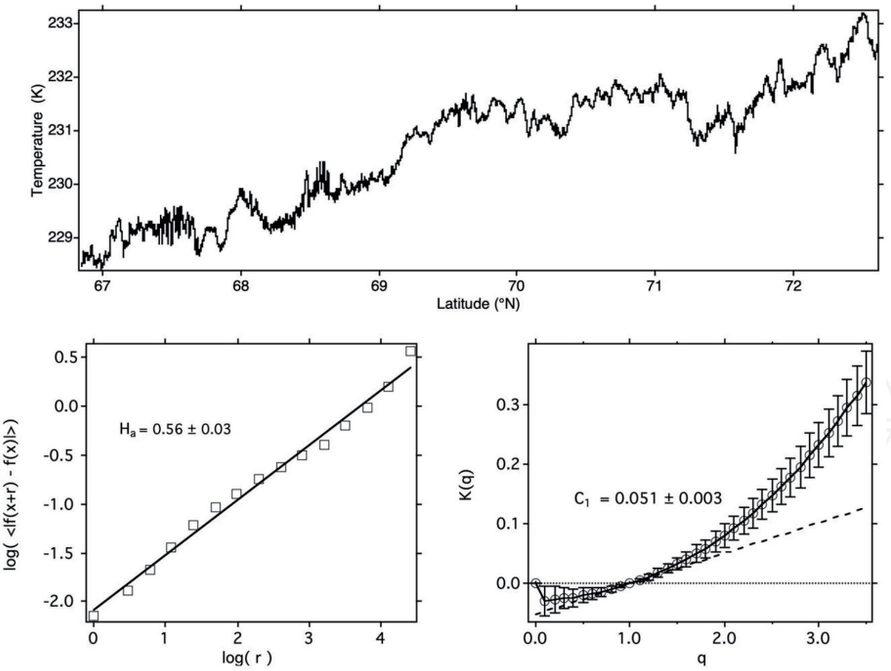

Figure 1.
Temperature on an approximately horizontal flight leg of 4700 seconds from (65°N,148°W) on a great circle to the NE, on 19970506 (yyyymmdd). The data are averaged to 5 Hz, or about 40 m horizontal resolution (top). Lower left, log–log plot to determine Hurst exponent H_1*; the value of 0.56 ± 0.03 confirms the theoretical value of 5/9 predicted by statistical multifractal theory (the flights combine both horizontal and vertical motion). Lower right, intermittency* $C_1(T)$*, which correlates with the mean* T *for the segment when the data for all suitable flight legs are so plotted.* $C_1(T)$ *is also correlated with the ozone photodissociation rate, see text and* ***Figures 3*** *and* ***4****.*

molecular populations in an asymmetric environment, following the molecular dynamics calculations of Alder & Wainwright [11], as taken up by Tuck [5, 12–14, 17]. In the atmosphere, it is driven by the Gibbs free energy arising from the entropy difference between the incoming organised beam of solar photons and the outgoing less organised flux of infrared photons over the whole 4π solid angle.

The statistical multifractal analysis is briefly outlined as follows.

It has been argued recently that G is computable from observations in a scale invariant medium, and shown to work [5, 14]:

$$G \equiv -\frac{K(q)}{q} \tag{1}$$

where $K(q)/q$ is a scaling quantity related to partition function f, Boltzmann constant k and temperature T by:

$$T \equiv \frac{1}{kq} \tag{2}$$

$$f \equiv \exp\{-K(q)\} \tag{3}$$

The relationship of $K(q)$ to the Hurst exponent H is given in Tuck [14] as.

$$H = H_q + K(q)/q \tag{4}$$

where

$$H_q = \frac{\zeta(q)}{q} \tag{5}$$

Quantity in Eqs. (1)-(5)	Statistical thermodynamics	Scaling equivalent
Temperature	T	$1/qk_{\text{Boltzmann}}$
Partition function	f	$e^{-}K(q)$
Energy	E	γ
Entropy	$-S(E)$	$c(\gamma)$
Gibbs energy	$-G$	$K(q)/q$

Table 1.
Equivalence between statistical thermodynamic and scaling variables.

and $\zeta(q)$ is the linear slope of a log–log plot of the first order structure function of the fluctuations of the observed variable versus a lag parameter covering the range of the variable. The Hurst exponent H, the intermittency C_1 and the Lévy exponent α are the scaling exponents that comprise the statistical multifractal description of atmospheric variability. Their derivation can be found in [14], with their statistical thermodynamic equivalences in **Table 1**.

By applying scale invariance to the bulk medium, and separately to the micro-droplet, the ΔG between the two may be obtained by difference. Application of high-resolution experimental and imaging techniques would then enable a comparison with the values obtained by quantum statistical methods applied to the reactant molecules [5]. The technique has been successfully applied to the air itself [14].

3. Some consequences of atmospheric statistical multifractality

As observed, atmospheric variables display the fat-tailed probability distribution functions characteristic of statistical multifractality; the Gaussians associated with Einstein-Smoluchowski diffusion are conspicuous by their absence. An example for temperature is shown in **Figure 2**.

The results from Alder and Wainwright [11] combined with statistical multifractal analysis [5, 12, 13, 17] imply that the air is not at chemical equilibrium and consequently the gas constant R is not sufficient to describe the molecular behaviour of the atmosphere. All current atmospheric models employ the gas constant in this manner. An experiment is suggested to test this point: measure the populations of the rotational energy levels of the major constituents, N_2 and O_2 to see whether they are at equilibrium – populated according to the Boltzmann distribution – or not. Direct measurement of the probability distribution of air molecule velocities would be a significant advance and check on the theory. The temperature should be compared between that consistent with Eq. (2) and that necessary to account for the rotational and translational populations. It is an important point that the implied higher population than Boltzmann equilibrium means that the far wings of the water vapour and carbon dioxide will be stronger than at equilibrium because these wings are caused by the molecular collisions with the highest speeds. That is where there is significant influence in calculations of the atmospheric radiative transfer, because unlike many line centres, they are not self-absorbed. There is observational evidence supporting this view of atmospheric temperature. **Figure 3** shows a plot of the ozone photodissociation rate $J[O_3]$, against the intermittency of temperature, $C_1(T)$, for flights in the lower Arctic stratosphere in the summer of 1997 and in the winter of 2000.

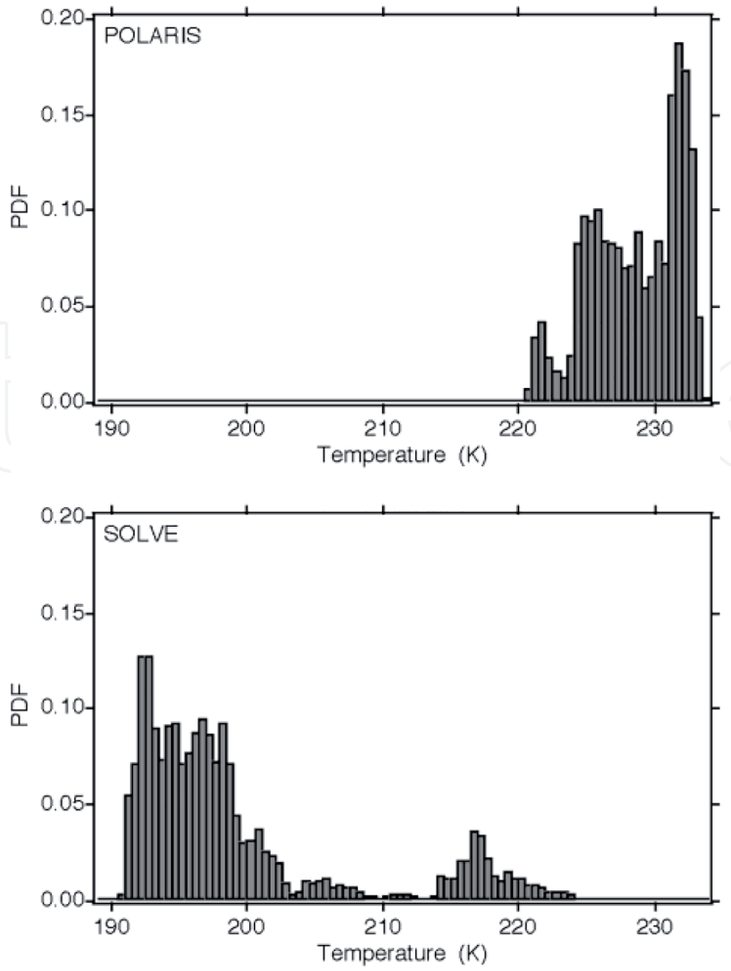

Figure 2.
Probability distribution functions (PDF) of temperature from ER-2 flights at 18–20 km in the Arctic April–September 1997 (top) and January–march 2000 (bottom). The millions of data points are averaged to 1 Hz, corresponding to approximately 200 m horizontal resolution. Note the long or fat tails; Gaussians are not seen.

The correlation is consistent with the effects of translationally hot oxygen atoms from ozone photodissociation being unequilibrated and conveying this to the air molecules as a whole. **Figure 4** shows the average temperature against intermittency $C_1(T)$ for the flight leg, and the correlation persists.

The reason for this, and the theoretical explanation, is in Chapter 5.1 of reference [12] and Section 4.2 of [14]. Further discussion is given in the next section. There are no suitable observational data to apply this analysis in the troposphere.

Now we consider the effects of scale invariance and statistical multifractality on clouds and aerosols. This approach was pioneered by Schertzer and Lovejoy [8, 9] and described at length in the context of clouds and radiation in Lovejoy and Schertzer [7]. Both phenomena pose major problems for current general circulation models (GCMs) that are used to attempt predictions of the future evolutions of climate. Lovejoy [10] has demonstrated that such models do not predict climate, they predict macroweather, the fluctuations on scales from 10 days to 30 years. 10 days is the approximate time for air to circle the globe, and it shows the scaling expected, namely 23/9 dimensional statistical multifractality. On time scales longer than 30 years, the data show similar scaling. On the intermediate 10-day to 30-year scale, the observations scale differently, and constitute the macroweather scale, which is what the so-called climate models predict. Macroweather forecasting of course has potential utility, but it is not climate prediction.

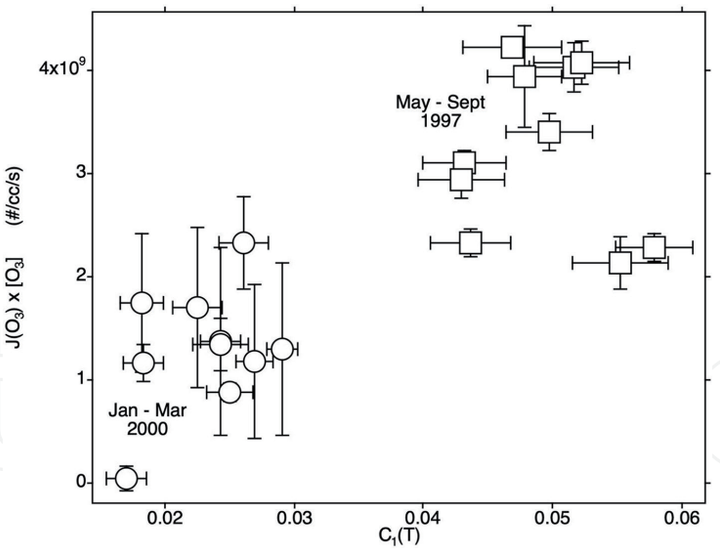

Figure 3.
For all suitable ER-2 flights April–September 1997 and January–march 2000. J*[O_3] on the ordinate,* C*$_1$*(T) *on the abscissa. The ozone photodissociation rate is averaged over the flight leg, with vertical bars representing the standard deviation. The intermittency of temperature is derived from the slope of the curve for each flight leg, see* ***Figure 1****, bottom left. The horizontal bars are the standard error of the slope of the line fit.*

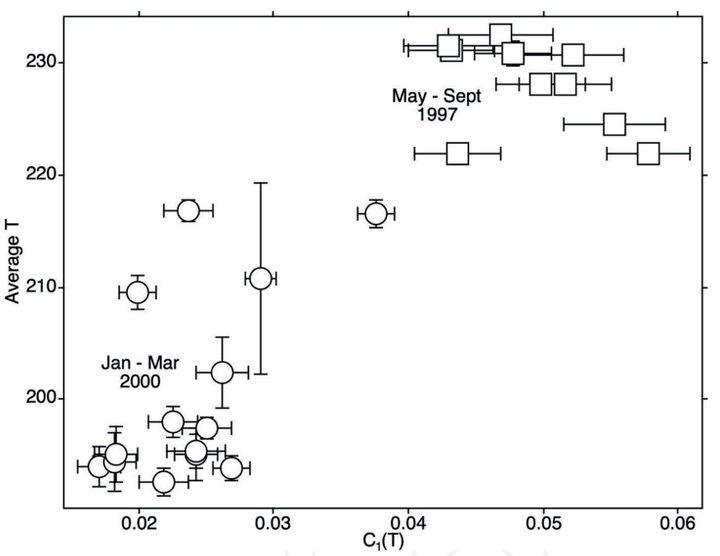

Figure 4.
As for ***Figure 3****, but with* T *averaged over the flight leg on the ordinate. The macroscopic temperature is proportional to the mean square velocity of the air molecules, supporting the suggestion that translationally hot photofragments from ozone photodissociation account for the correlations in* ***Figures 3*** *and* ***4****.*

Clouds are still a major uncertainty in any modelling, because they involve the physical chemistry of all three phases of water, the complex chemistry of gas-to-particle conversion, the role of aerosols of varying sizes in acting as condensation nuclei, particularly as regards the role of organic surfactants. All of these phenomena affect the transmission of radiation, both UV/visible and infrared. The altitude of the clouds is also critical, via their temperature and hence state. As an example, we note that the organic content of lower stratospheric aerosols plays a disproportionately large role in their radiative influence [18]. This whole area of aerosols, clouds and radiation needs examination by scale invariant techniques, from individual particles to cloud decks. The scale invariant Gibbs free energy is, we argue, an appropriate tool. Its effects are of course intimately related to atmospheric temperature and its maintenance via dissipation through intermolecular energy exchange and subsequent infrared radiation to space.

4. Atmospheric temperature

Before considering the role of Gibbs free energy in the atmosphere, we take a detailed look at a sample of evidence from aircraft flights, drawing on a selection of figures from Tuck [12–14, 17, 19] to examine what processes determine atmospheric temperature. The discussion starts with **Figures 1–4**, taken from reference [17], and questions and answers in [20].

Figure 1 shows a temperature trace, and the plots for obtaining the Hurst exponent H_1 and the intermittency C_1 from it. It is a great circle flight in the lower stratosphere during Arctic summer. The value $H_1 = 0.56 \pm 0.03$ is observational confirmation of the theoretical value of 5/9 posited by the statistical multifractal equations of Lovejoy and Schertzer [7], in the case of temperature behaving like a passive scalar in the horizontal. We will see, however, that T does not always so behave in the vertical. Further evidence of statistical multifractal behaviour can be seen in **Figure 2**, where the probability distributions are shown for millions of points from ER-2 flights taken at 1 Hz – corresponding to 200 m horizontal resolution - during Arctic summer and winter conditions. The fat tails are characteristic; Gaussians are not seen. The Lévy exponent α expresses this, being on average 1.6 whereas a Gaussian has the value 2; its predicted range is $1.5 < \alpha < 2$, see [12, 13]. The implication of this is that the variance of T does not converge, although the mean does.

The evidence for correlations between ozone photodissociation rate with temperature and its intermittency is exemplified in **Figures 5** and **6**.

Figure 3 shows the photodissociation rate $J[O_3]$ plotted against the intermittency of temperature $C_1(T)$ for flights of the ER-2 in the Arctic lower stratosphere for the spring–summer-autumn of 1997 and the winter of 2000. **Figure 4** shows T itself plotted against $C_1(T)$ for the same data. We examine in **Figures 5** and **6** evidence from a particular flight, 19970509 (yyyymmdd), which crossed the terminator in a region of low wind speeds, enabling flight in 'the same air mass' in sunlit and dark conditions. The separate sunlit and dark legs were not long enough for a separate statistical multifractal analysis. The flight was 35 days from summer solstice and had a higher sun than most of the flights on **Figures 3** and **4**. In **Figures 3** and **4**, the intermittency of temperature never drops to zero even when the ozone photodissociation rate does, although approaching it in the coldest and darkest points in winter; see the points in the lower left corners. The intermittency of temperature

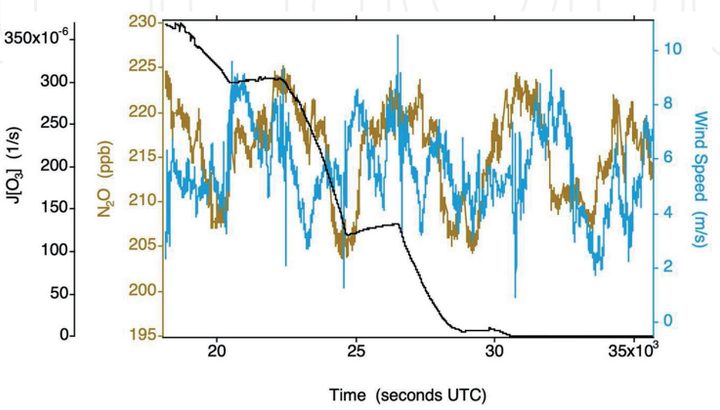

Figure 5.
Observations from the ER-2 on 19970509 (yyyymmdd), when 'racetrack' segments were flown either side of the terminator in a slow moving airmass at about 55 mbar. Black curve, $J[O_3]$; O_3, blue; T, *red; green, east longitude. Note that temperature is cooler in the dark, while ozone does not change. Like wind speed and the tracer nitrous oxide in* ***Figure 6****, it is approximately symmetrical about the terminator, where* $J[O_3] \approx 0$. T *has increased by about 0.4 K in two hours in the sunlit air.*

is highest in the sunniest and warmest points, clustered in the upper right corners of **Figures 3** and **4**. **Figures 5** and **6** can cast some light on the foregoing results, allowing a direct estimate of the radiative heating rate.

In **Figures 5** and **6**, the black trace defines $J[O_3]$ and hence goes to near zero at the terminator and beyond into night. Across the terminator, the low wind speed, ozone and tracer nitrous oxide, while varying about a mean in sunlight and dark, remain constant on average. That is not true of temperature, which is on average 0.4 K higher in sunlit conditions, 'in the same air'. A heating rate of 0.2 K/hour at 55 mbar can be calculated, and successfully checked by computation of the energy influx from radiation and the specific heat of air. The heating rate is consistent with the observation of $J[O_3]$.

In May, and September, the temperature in the sunlit part of the flight legs was on the warm side of the probability distribution compared to the dark side, again 'in the same air'. This result can be seen in **Figures 7** and **8**.

These considerations are also consistent with the concept of heating by unthermalized translationally hot oxygen atoms causing intermittency of temperature.

The behaviour of temperature in the vertical is not that of a well-mixed passive scalar ('tracer' in atmospheric usage). Its scaling is dominated by gravity [12, 13, 21–23]. Experimental evidence is shown in **Figures 9** and **10**.

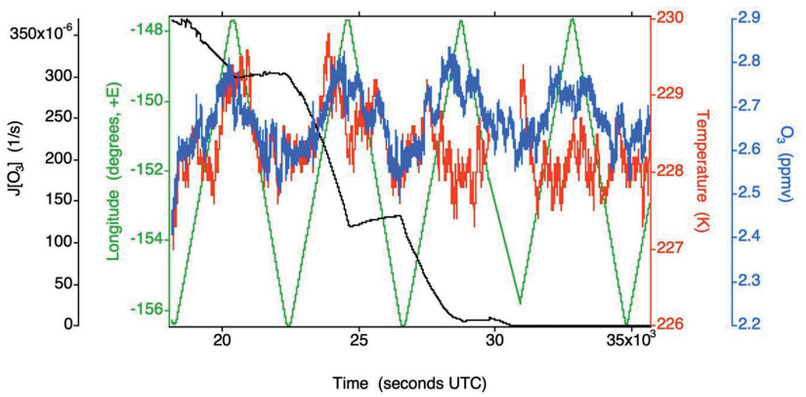

Figure 6.
Same flight as in ***Figure 5****. Windspeed, light blue; nitrous oxide, brown. In a slow-moving air mass (no more than 3% movement during the flight), wind speed and tracer are approximately symmetrical about the terminator, with temperature in* ***Figure 5*** *being the only variable showing asymmetry about* $J[O_3] \approx 0$.

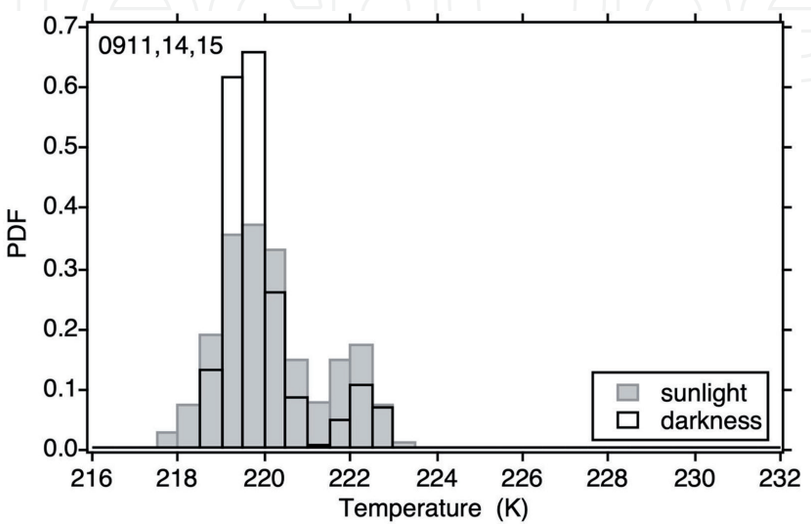

Figure 7.
Probability distribution for temperature, normalised to unity, for the data in ***Figure 5****. Population has moved from the more probable values on the dark side of the terminator to the sunlit side.*

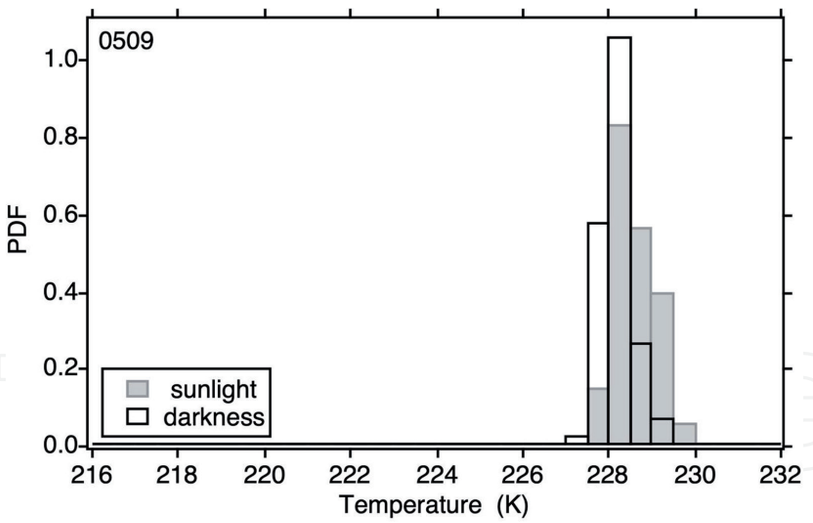

Figure 8.
Probability distribution for temperature, normalised to unity, either side of the terminator for three flights from (65°N,148°W) 19970911 (yyyymmdd), 19970914 (yyyymmdd) and 19970915 (yyyymmdd). As for 20040305 (yyyymmdd), the sunlit data have gained population from the dark data.

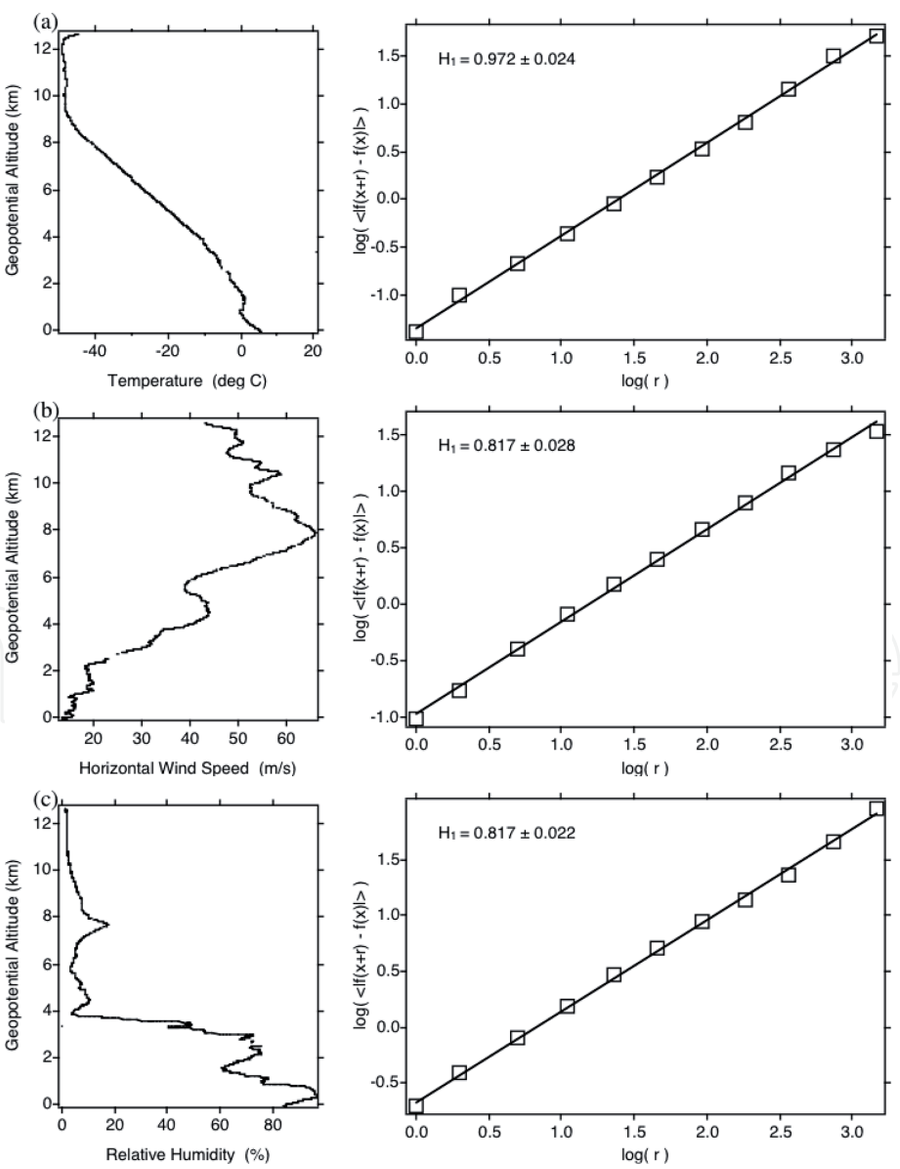

Figure 9.
Observations and H_1 *scaling for dropsonde descent at (42° 42′ 56” N, 170° 55′ 30” W), temperature, horizontal wind speed and relative humidity, 20040305.*

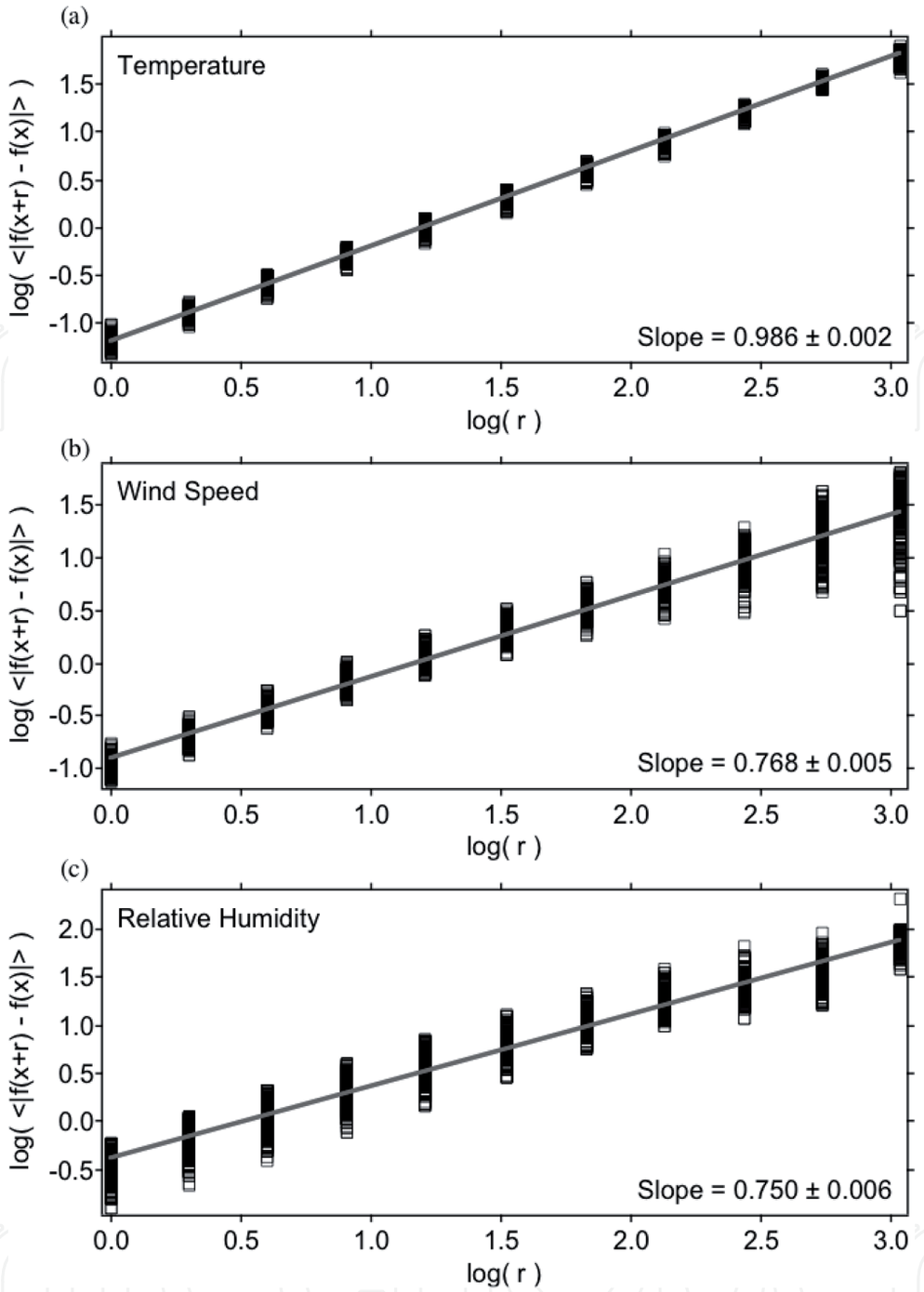

Figure 10.
Composite variogram for all 885 useable dropsonde descents over the eastern Pacific Ocean, from 15°N to 60°N, like that in ***Figure 9*** *during winter storms 2004, 2005 and 2006. The scaling is excellent for all three of temperature, horizontal wind speed and relative humidity. See [23] for further discussion.*

Figure 9 shows the vertical scaling of the temperature, horizontal wind speed and relative humidity for an individual dropsonde descent in early March 2004 [23]. The scaling exponent of temperature $H_1(T)$ is near unity; it does however have significant intermittency of ≈ 0.20 (not shown), demonstrating departures from hydrostatic equilibrium. The vertical scaling exponents $H_1(s)$ and $H_1(\mathrm{rh})$ of horizontal wind speed and relative humidity are significantly less than that of temperature, being not directly affected by gravity, unlike the total air density and hence temperature. **Figure 10** shows the grand average composite variogram of 885 dropsondes from the three years of Winter Storms 2004, 2005 and 2006. The vertical scaling of temperature, wind speed and relative humidity is further discussed in [23].

5. Gibbs free energy, irreversibility, the atmosphere and climate heating

Gibbs free energy – 'exergy' – is what enables, via dilution of energy density, the circulation of the atmosphere. It forces directional evolution through the most energetic high-speed molecules, giving the arrow of time to the atmosphere, and its associated irreversibility. Its 2nd Law cost is paid for by the dissipation enabled by the molecules with the most probable speeds easily exchanging energy to maintain an operationally observed temperature while enabling the evolution of vorticity and atmospheric flow, expressed as scale invariant turbulence. The basis for this is discussed in Chapter 7 of Tuck [12], arising from Alder and Wainwright [11]. The energy source is the solar beam, the dissipation is infrared dissipation to space from the infrared active molecules, mainly but not exclusively in the 7–14 μm wavelength window region, by water vapour, water vapour dimers, carbon dioxide, ozone, methane, nitrous oxide and halocarbons. These radiatively active molecules display scale invariance, ensuring that the absorption and emission of radiation operates on all scales, from the mean free path up to 15 orders of magnitude to a great circle. The long-understood fact that atmospheric state and evolution is governed by the interaction between radiation, chemistry and dynamics is extended to the smallest, microscopic scales. The transition from meso to macro scales maintains an operational temperature, and points to the reason the atmosphere 'integrates' a portion of the variability in its constituents and dynamical quantities [14].

Because the change in Gibbs free energy ΔG is equal to or is less than the difference between the change in enthalpy H and the product of the temperature T change and the entropy S change,

$$\Delta G \leq \Delta H - T\Delta S \tag{6}$$

a thermodynamic profit in the case of amelioration of climate heating by fossil fuel burning is not possible by using power generated by those means. Consider that typical coal burning power stations operate at about 35% efficiency; 65% is dissipated. It follows that the entropy cost of any remedial intervention must be paid for by energy derived from renewable sources rather than from fossil fuel combustion. For example, the entropy cost of removing 25% of 400 ppm mole fraction of carbon dioxide from the air will be very high. **Figure 11** shows the behaviour of the Gibbs free energy derived from scaling analysis of the temperature in **Figure 1**, see [14].

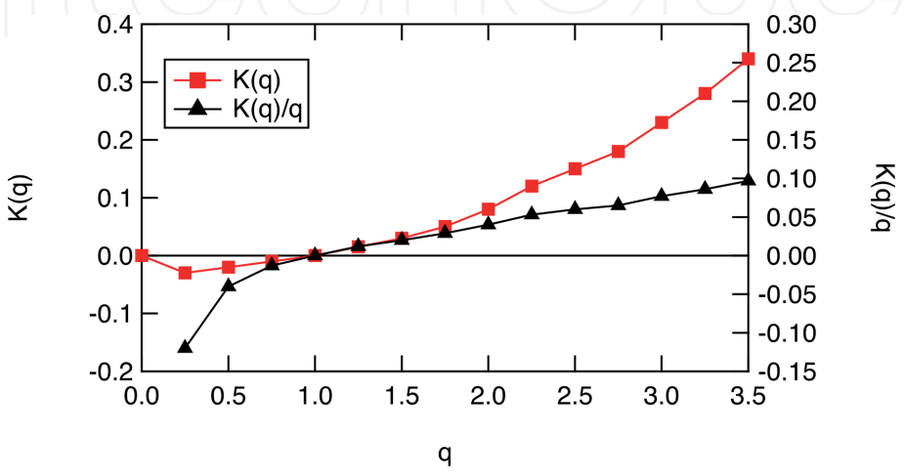

Figure 11.
The behaviour of K(q) *and* K(q)/q *as a function of* q; *see* ***Table 1*** *and Eqs. (1)-(5) for definitions. At* q = 1 *both functions are at or near zero, indicting a steady state condition. There is further discussion in Section 4 of [14].*

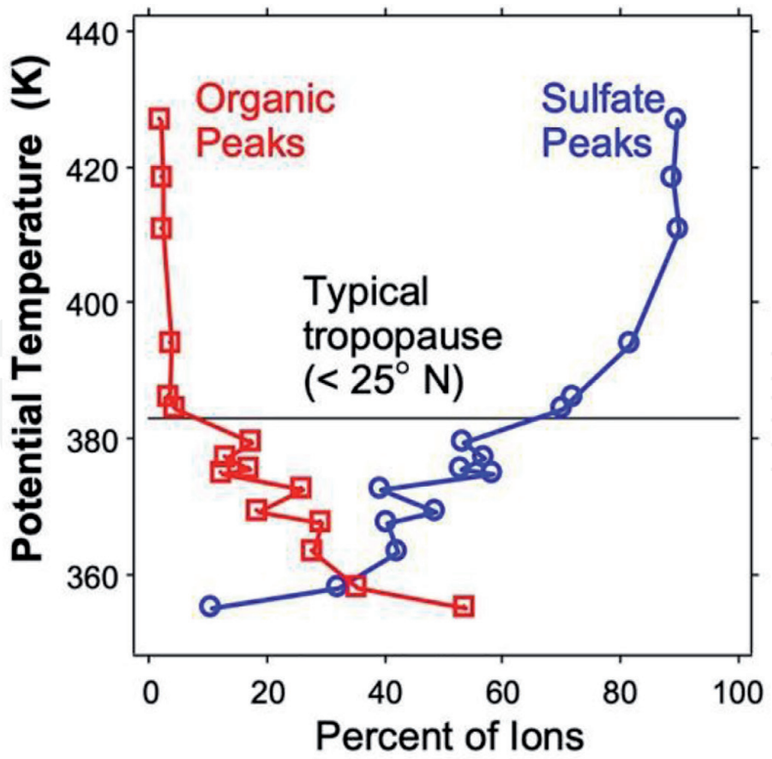

Figure 12.
The relative percentages of organic and sulfate ions in the single particle laser mass spectrometry from the WB57F aircraft [24]. There is significant presence of organic molecules well into the stratosphere. See also [18, 19, 25].

Both Gibbs free energy $K(q)/q$ and the exponent in the partition function $-K(q)$ go through zero at $q = 1$, indicating existence at or near a steady state. Input energy will move the system from steady state towards higher temperatures, with scaling Gibbs free energy enabling movement to more energetic states as $K(q)/q$ becomes more negative. Cooling on the other hand will move the system to less energetic steady states at higher q.

The above considerations apply to geoengineering projects. Further considerations apply in the case of so-called "solar radiation management", such as the limitations of our current understanding of the chemical, radiative and cloud physical roles of aerosols in the lower stratosphere [5, 12, 18, 19]. Aerosols have been shown, over a population of millions of individual particles, to contain 45 different elements from the 92 in the periodic table, not all of course in any single particles. The aerosols are neither internally nor externally mixed at altitudes 5 to 19 km [24].

The organic content of lower stratospheric aerosols has significant effects on radiative transfer [18] and is photochemically influenced [19, 25] (see **Figure 12**).

The advantage of the statistical multifractal approach embodied in Eqs. (1)-(5) is that it can be computed for the system as a whole with adequate observations of wind speed, temperature and if necessary the radiative constituents to use Eq. (6), without having to measure all the chemical constituents of air to make what are in any case inadequate equilibrium quantum statistical thermodynamic calculations. It could also be applied to individual aerosol particles [5] via high-resolution observations and molecular dynamics calculations. These arguments, and those in the preceding sections, suggest a programme of future research.

6. Conclusion

The above arguments show that the changes from fossil-fuel induced heating are irreversible in the strict sense of quantum statistical thermodynamics. This however

is expected because the atmosphere is not an isolated system at equilibrium; rather it is an open system far from equilibrium. We show above that it is irreversible by statistical multifractal analysis; **Figure 11** is an example of how it works, showing that to move from an existing steady state will take energy to do work that must be enabled by the dissipation mechanism, which is infrared radiation to space. Conditions to achieve a thermodynamic profit therefore indicate that any remedial action must use renewable energy, which in principle is available in abundance given that the entire biosphere uses only about 1% or so of the incident solar beam. The many uncertainties in climate modelling; in the cloud physical, chemical, dynamical and radiative uncertainties associated with aerosols; in the inability to forecast beyond macroweather time scales all imply that geoengineering, particularly in the form of "solar radiation management", is an extremely uncertain gamble [19]. While the situation is in principle irreversible as the entropy-carrying infrared photons recede into space at the speed of light over the whole 4π solid angle, the simplest and least risky course of action is to use renewably generated Gibbs free energy to move to a sustainable steady state, by reducing and then eliminating fossil fuel burning, and to do it with despatch.

Acknowledgements

Interaction and cooperation with Aiden Hovde, Shaun Lovejoy, Daniel Schertzer and Veronica Vaida have been essential in developing the case presented here.

Author details

Adrian F. Tuck
Atmospheric Physics, Imperial College London, UK

*Address all correspondence to: adrianftuck@gmail.com

References

[1] Donaldson DJ, Vaida V. The Influence of Organic Films at the Air-Aqueous Boundary on Atmospheric Processes. Chemical Reviews 2006; 106(4) 1445-1461.

[2] Yan X, Bain RM, Cooks, RG. Organic Reactions in Microdroplets. Angewandte Chemie International Edition 2016; 55 12960-12972.

[3] Nam I, Lee JK, Nam HG, Zare RN. Abiotic Production of Sugar Phosphates and Uridine Ribonucleoside in Aqueous Droplets. Proceeding of the National Academy of Sciences of the United States of America 2017; 114 12396-12400.

[4] Zare RN. Chemical and Engineering News 2018. Available on line: https://www.cen.acs.org/sponsored-content/what-will-be-chemistrys-next-big-thing.html (accessed 27 May 2018).

[5] Tuck AF. Gibbs Free Energy and Reaction Rate Acceleration in and on Microdroplets, Entropy 2019; 21 1044.

[6] Wilson KR, Prophet AM, Rovelli G, Willis MD, Rapf RJ, Jacobs MI. A Kinetic Description of how Interfaces Accelerate Reactions in Micro-compartments. Chemical Science 2020; 11 8533-8545.

[7] Lovejoy S, Schertzer D. The Weather and Climate: Emergent Laws and Multifractal Cascades. Box 5.1 pp 127-128. Cambridge: Cambridge University Press; 2013.

[8] Schertzer D, Lovejoy S. Generalised Scale Invariance in Turbulent Phenomena. Physico-Chemical Hydrodynamics Journal 1985; 6 623-635.

[9] Schertzer D, Lovejoy S. Physical Modeling and Analysis of Rain and Clouds by Anisotropic Scaling of Multiplicative Processes. Journal of Geophysical Research 1987; 92 9693-9714.

[10] Lovejoy S. Weather, Macroweather, and the Climate. Oxford: Oxford University Press; 2020.

[11] Alder BJ, Wainwright TE. Decay of the Velocity Autocorrelation Function. Physical Review A: Atomic, Molecular and Optical Physics 1970; 1 18-21.

[12] Tuck AF. Atmospheric Turbulence: a Molecular Dynamics Perspective. Oxford: Oxford University Press; 2008.

[13] Tuck AF. From Molecules to Meteorology via Turbulent Scale Invariance. Quarterly Journal of the Royal Meteorological Society 2010; 136 1125-1144.

[14] Tuck AF. Proposed Empirical Entropy and Gibbs Energy Based on Observations of Scale Invariance in Open Nonequilibrium Systems. Journal of Physical Chemistry A 2017; 121 6620-6629.

[15] Goede APH, Tuck A, Burrows JP, Fischer H, Leisner T, Beekmann M, Flaud J-M, Paretzke H, Suppan P, Baier F, Hamacher T, Platt U, Zanis P. Energy and Environment: The Intimate Link. Verhandlungen der Deutschen Physikalischen Gesellschaft, Frühjahrstagung 2008; Umweltphysik Reihe VI Band 43, 311.

[16] Lovejoy S, Schertzer D, Stanway JD. Direct Evidence of Multifractal Cascades from Planetary Scales Down to 1 km. Physical Review Letters 2001; 86 5200-5203.

[17] Tuck AF, Hovde SJ, Richard EC, Gao R-S, Bui TP, Swartz WH, Lloyd SA. Molecular Velocity Distributions and Generalized Scale Invariance in the Turbulent Atmosphere. Faraday Discussions 2005; 130 180-193.

[18] Yu P, Murphy DM, Portmann RW, Toon OB, Froyd KD, Rollins RW, Gao R-S, Rosenlof KH. Radiative Forcing from Anthropogenic Sulfur and Organic Emissions Reaching the Stratosphere. Geophysical Research Letters 2016; 43 9361-9367.

[19] Tuck AF, Donaldson DJ, Hitchman MH, Richard EC, Tervahattu H, Vaida V, Wilson JC. On Geoengineering with Sulphate Aerosols in the Upper Tropical Troposphere and Lower Stratosphere. Climatic Change 2008; 90 315-331.

[20] Duxbury G, Tuck AF, Platt U, Heard DE, Ashfold MNR, Plane JMC, Herrmann H, Jones RL, Smith IWM, Taatjes CA. General Discussion. Faraday Discussions 2005; 130 248-252.

[21] Lovejoy S, Tuck AF, Hovde SJ, Schertzer D. Do Stable Atmospheric Layers exist? Geophysical Research Letters 2008; 35 L01802.

[22] Tuck AF, Hovde SJ. Fractal Behavior of Ozone, Wind and Temperature in the Lower Stratosphere. Geophysical Research Letters 1999; 26 1271-1274.

[23] Hovde SJ, Tuck AF, Lovejoy S, Schertzer, D. Vertical Scaling of Temperature, Wind and Humidity Fluctuations: Dropsondes from 13 km to the Surface of the Pacific Ocean. International Journal of Remote Sensing 2011; 5891-5918.

[24] Murphy DM, Thomson DS, Mahoney MJ. In situ measurements of organics, meteoritic material, mercury and other elements in aerosols from 5 to 19 kilometers. Science 1998; 282 1664-1669.

[25] Ellison GB, Tuck AF, Vaida V. Atmospheric Processing of Organic Aerosols. Journal of Geophysical Research 1999; 104 11633-11641.